Materials Research Express



**PAPER** • **OPEN ACCESS**

# Comparison of the mechanical properties of amorphous FeSiB and FeGaSiB films

To cite this article: Qayes A Abbas *et al* 2025 *Mater. Res. Express* **12** 096403

Materials Research Express



OPEN ACCESS

RECEIVED
9 May 2025

REVISED
5 August 2025

ACCEPTED FOR PUBLICATION
5 September 2025

PUBLISHED
15 September 2025



PAPER

# Comparison of the mechanical properties of amorphous FeSiB and FeGaSiB films

**Qayes A Abbas**[1,2], **Zhaoyuan Leong**[2], **Saturi Baco**[3] **and Nicola A Morley**[2,*]

[1] Department of Physics, College of Science, University of Anbar, Anbar, Iraq
[2] School of Chemical, Materials, and Biological Engineering, University of Sheffield, Mappin Street, S1 3JD, United Kingdom
[3] Programme of Industrial Physics, Faculty of Science and Natural Resources, Universiti Malaysia Sabah, Jalan UMS, 88400 Kota Kinabalu, Sabah, Malaysia
[*] Author to whom any correspondence should be addressed.

**E-mail:** n.a.morley@sheffield.ac.uk

**Keywords:** amorphous thin films, nanoindention, mechanical properties

## Abstract

As technology gets smaller, the need to understand how the mechanical as well as functional properties of thin magnetic films change as a function of thickness and substrate is required. This then allows for better material selection for applications, as thin amorphous and nanocrystalline magnetic films are used in micro-electromechanical systems (MEMS), such as actuators, field and strain sensors. This work used the nanoindentation technique to study the mechanical properties (hardness, Young's modulus and yield strength) of amorphous FeGaSiB and FeSiB thin films to determine how the thickness, substrate and composition influence these properties. Along with understanding how the addition of Ga changed the amorphicity of the films with thickness. It was found that the Young's Modulus and hardness decreased by ∼15% with the addition of Ga, plus the films were less elastic compared to the FeSiB films. The yield strength was 30% higher for the films grown on glass compared to silicon, while the hardness and Young's modulus of both FeSiB and FeGaSiB films increased with decreasing film thickness. Further, these results helped to gain understanding on the role of film thickness to the amorphicity of the film.

## 1. Introduction

Technology is rapidly getting smaller and smaller, with micro-electro-mechanical systems (MEMS) devices such as sensors and actuators now incorporating nano-scale structures and designs. Sensors such as field and strain types, both use magnetostrictive thin films within their design [1, 2]. How the functional properties such as magnetostriction constant and saturation magnetization change with film thickness is well documented [3–5], but less work has been done on how the mechanical properties, such as Young's modulus and hardness change with thickness, and how much the substrate influences these mechanical properties. To fully utilize magnetostrictive films in applications, a full understanding of the structural, magnetic and mechanical properties is required. One form of magnetostrictive film often used in the applications have an amorphous morphology [6], as they tend to have good magnetostriction constants [7, 8], along with the excellent soft magnetic properties required for the sensing applications. For example, in [9], the authors showed that by controlling the residual stress-state within amorphous FeSiB films, the films could be used for stress impedance sensing systems. While in [10], they looked at the inductance behaviour of thicker FeSiB films under tensile loading for the development of a micro force sensor. Further FeSiB films have been used within sensors to detect highly contagious diseases within a flexible magnetoelastic composite film [11] and within laminated magnetoelastic heterostructures used in magnetic field sensors to map the magnetic field of the heart [12]. These magnetoelastic heterostructures [12, 13] are being designed for applications such as wearable antennas and tuneable inductors, using the coupling between piezoelectric layers and magnetostrictive films, including

FeGa [14], FeGaB [15, 16] and FeSiB [17]. The magnetostrictive films within these devices tend to be thicker than 500 nm, and used on flexible substrates, hence the mechanical properties become of interest.

The majority of the research on the mechanical properties of amorphous magnetic alloys has been done on melt-spun ribbons [18–20]. Lashgari *et al* [19] studied the mechanical properties of amorphous as-grown and heat treated $Fe_{80.75}Si_8B_{11.25}$ ribbons. They found that the heat treatment helped to increase the hardness from 10 GPa to 11.2 GPa and increased the reduced elastic modulus from ~160 GPa to ~238 GPa. Further they studied the addition of Cu to FeSiB ribbons [20], along with the annealing temperature. For the as-spun amorphous ribbons, the hardness and the reduced elastic modulus decreased with the increased addition of Cu into the ribbon from 12 GPa to ~10 GPa and ~120 GPa to ~60 GPa respectively. After annealing, crystallites started to form in the ribbons, which lead to an increase in hardness by over 35% and in the reduced elastic modulus by over 40% for all the samples studied.

For thin magnetostrictive films, Jen *et al* [21] studied the mechanical properties of polycrystalline 250 nm $Fe_{81-x}Co_xGa_{19}$ ($0 \leqslant x \leqslant 19$) films grown on Corning 0211 glass. They determined that the hardness of the films increased from 6.5 GPa ($x = 0$) to 7.7 GPa ($x = 11$) with the addition of Co, then decreased with further Co concentration. While the Young's modulus decreased with increasing Co concentration from 130 GPa ($x = 0$) to 115 GPa ($x = 7$), then increased again up to 140 GPa with further Co addition. No discussion on the substrate influence was given. Baco *et al* [22] investigated the mechanical properties of polycrystalline 600 nm $FeCoCr_x$ ($0 \leqslant x \leqslant 9$) films grown on silicon substrates. They found that their films were thick enough, such that the silicon substrate did not influence the mechanical properties. They also determined that the addition of Cr to FeCo decreased the Young's modulus from 167 GPa ($x = 0$) to 156 GPa ($x = 7.2$) and decreased the hardness from 14.8 GPa ($x = 0$) to 12.2 GPa ($x = 7.2$), but did increase the yield strength by 20%. While Nicolenco *et al* [23] investigated the mechanical properties of magnetostrictive Fe-Ga films, as a function of Ga concentration, and determined that the reduced elastic modulus and hardness both decreased with increasing Ga content. For example, the 2% Ga film had a hardness of 5 GPa and reduced modulus of 134 GPa, while the 15% Ga film the hardness was 3.35 GPa and the reduced modulus was 128 GPa. Other work on the mechanical properties of magnetic thin films, includes studies on the shape memory alloy, Ni-Mn-Ga [24, 25], which investigated the localised plastic deformation on the martensitic transformation [25] and found the thickness strongly influenced the pseudoelastricity and the bulk martensitic transformation [24]. While investigations into soft magnetic thin films such as CoFeDy [26], and CoFeSm [27], determined the hardness of these film decreased with increasing film thickness.

The motivation for adding Ga atoms, which have a nonmagnetic property, within FeSiB films included: i. to decrease the magnetization of these films to be suitable for use them in low magnetic field sensors, which has been done in previous work [28], ii, to produce new type of magnetic films and study their properties, which was achieved previously [29], and iii, to study the effect of Ga on the magnetostriction coefficient [29], which depends on the magnetoelastic and elastic coefficients. For these films to be used within applications such as low magnetic field sensors, it is important to study the mechanical properties to determine whether Ga causes any detrimental problems, along with any links to their magnetic properties.

Previous work has focused on the structural and magnetic properties of amorphous FeSiB and FeGaSiB thin films [28, 29], where it was determined that the addition of Ga did not change the morphology but increasing the Ga concentration decreased the magnetization by 10%. Both sets of films had soft magnetic properties as a function of film thickness and Ga concentration. While the magnetostriction constant decreased with increase in thickness for the FeSiB films, it remained roughly constant for the FeGaSiB films. Therefore, to gain a full understanding of these films for applications, the mechanical properties have been investigated using the nanoindentation technique. This work has studied how the film's thickness, composition and substrate influence the elastic modulus, hardness, and yield strength. These mechanical properties are important, as the Young's modulus of magnetic thin films is used within the calculation of the magnetostriction coefficient [30], which is the main property for MEMS strain sensors. While the yield strength gives an indication of the maximum stress that can be applied to the film before plastic deformation occurs. This again is important when designing MEMS devices.

## 2. Research hypothesis

As both FeSiB and FeGaSiB are amorphous, understanding the role of Ga in the alloying is important. Amorphicity in alloy systems can be understood through semi-empirical parameters such as the atomic size difference and enthalpy of mixing [30]. Biplots of atomic size difference can adequately describe the change in the structural stability of the system. In such a biplot, the regions of structural stability may be characterized and determined through statistical means such as cluster analysis [32]. One such example is the biplot (mixing enthalpy versus atomic size difference) shown in [33] where the centroids for each phase (amorphous, multi-

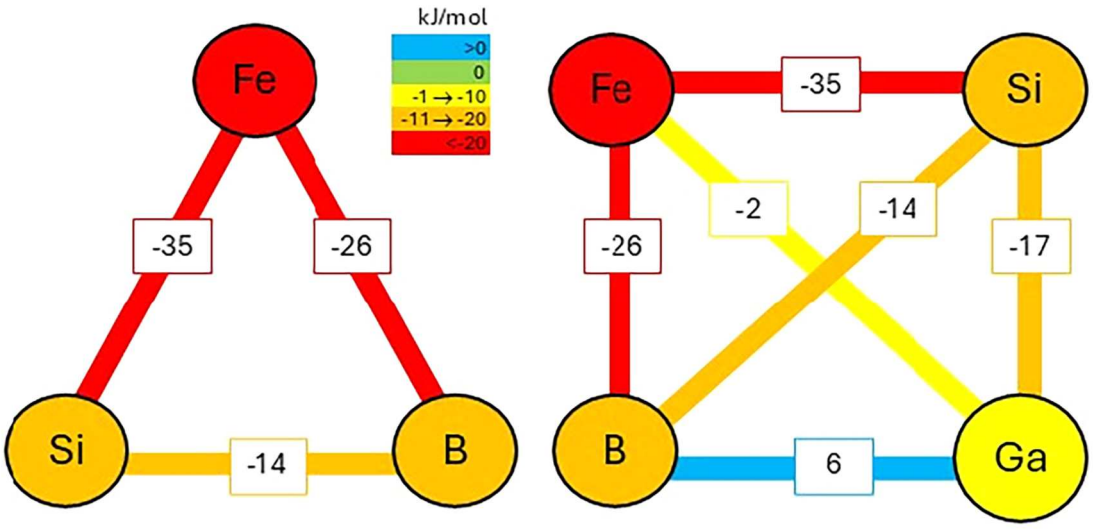


**Figure 1.** Enthalpy of mixing values for FeSiB and FeGaSiB [31]. The individual alloying elements are colour coded according to the average enthalpy of mixing values they have with the other elements.

phase, and single-phase) may be determined using the cluster analysis method. The coordinates the amorphous phase is ($-20$ kJ mol$^{-1}$, 12 ); the enthalpy of mixing of multi-component alloy (more than 2 components) can be approximated using the sub-regular solution model [31] while the atomic size difference can be obtained as defined in [34]. These values for FeSiB and FeGaSiB are ($-32.67$ kJ mol$^{-1}$, 0.205) and ($-22$ kJ mol$^{-1}$, 0.325) [16]. Considering that the centroid of the amorphous phase is ($-20$ kJ mol$^{-1}$, 12), it is reasonable to assume that the further away from this centroid an alloy sits in the biplot, the less amorphous it would tend to be. A Euclidean distance function was used to compute the distance away from the amorphicity cluster centre and for equimolar FeSiB and FeGaSiB it was found to be 17.31 and 22 units respectively. This means that FeSiB is more 'amorphous' than FeGaSiB. The individual enthalpy of mixing for each element pair is given in figure 1. It is observed that the Ga-B value is positive, meaning it is not a favourable mixing, and therefore may cause segregation of the elements within the film.

For thin films, an increase or change in structural stability can be achieved by judicious selection of the substrate in polymers [35] as well as alloys [36] by tuning the interfacial energy. According to classical nucleation theory [37], nucleation is driven by a driving force that can be characterized by the chemical potential—this chemical potential is intimately related to the enthalpy of mixing. Enthalpy of mixing values are more negative for amorphous-forming systems, and the chemical potential is higher for these systems as well, which means that sufficient entropy is required to maintain the amorphicity of the system (in the form of the atomic size difference as represented in the semi-empirical biplots).

Thus it stands to reason that: (1) Entropy reduces the further away from the energy providing edge. Therefore, a thicker film means that the top of the film would have a higher yield strength and hardness [38, 39] due to reduced crystallinity, *ceteris paribus*. (2) A more amorphous alloy system would have a lower change in hardness by varying thickness. To test this hypothesis, FeGaSiB and FeSiB film of different thicknesses and grown on different substrates were tested.

## 3. Materials and methods

All the films were fabricated using a co-sputter-evaporation deposition system [40], which allows control of the concentration of Ga within the films. Before growth, the substrates (either Si (100) or glass) were washed using acetone and isopropanol (IPA). For each film growth, three substrates were used and attached to a glass slide using polymethyl methacrylate (PMMA). The film thickness was monitored via the Fe rate monitor above the Fe gun within the sputter-evaporation chamber [40]. This gives a good estimate of the film thickness during growth, which is then measured after the growth. To determine the actual film thickness, a PMMA blob was placed on one substrate before deposition using a toothpick. After deposition, the PMMA blob was removed using acetone, to leave a sharp edge, allowing the film thickness to be determined using an atomic force microscopy (AFM). For both film sets, Metglas 2605SA1 foil with composition $Fe_{85}Si_{10}B_5$ was used as a sputter target. The FeSiB films were grown at a chamber pressure of 4 mbar, sputter power of 20 W and with the Ga evaporation set to off. While the FeGaSiB films were grown at the same sputter power (20 W) and chamber

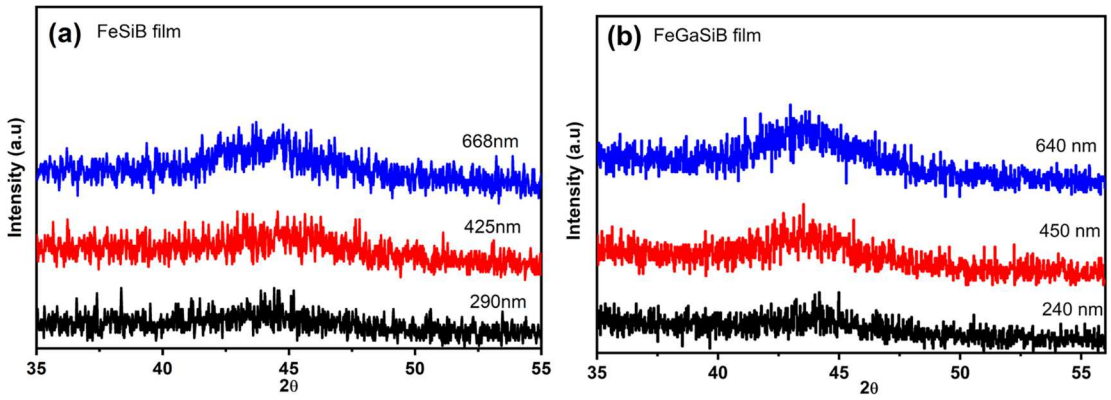


**Figure 2.** XRD of (a) FeSiB films and (b) FeGaSiB films for the different film thicknesses.

pressure (4 mbar), with the Ga being evaporated at a constant arbitrary rate of 0.2. From previous work [28, 29], these parameters gave the 'best' soft magnetic properties. For each composition, three different film thicknesses were fabricated. For the FeSiB films, these were 290 nm, 425 nm and 668 nm, and the FeGaSiB films, these were 240 nm, 450 nm, and 640 nm. The film thicknesses were chosen to be ~200 nm different to allow for any changes in the mechanical properties with thickness to be observed and to determine when the substrate stopped influencing the measurements. From previous work [22], it was determined that for 600 nm FeCoCr films, the silicon substrate did not influence the mechanical results, and therefore the thickest films studied in this work were thicker than 600 nm.

To verify the compositions of the films, x-ray photo spectroscopy (XPS) was used. The measurements were carried out on a Thermo Fisher Scientific NEXAS spectrometer, using a micro-focused monochromatic Al x-ray source, with energy 1486.6 e V and power 19.2 W, over an area of approximately 100 microns. The data were analysed at pass energies of 150 eV for survey scans and 40 eV for high resolution scans, with 1 eV and 0.1 eV step sizes respectively. For the FeSiB films, the composition was determined to be $Fe_{85}Si_7B_8$, and for the FeGaSiB films, it was $Fe_{82}Ga_7Si_5B_6$. The composition was determined by taking three measurements in three different places on the film surface area and then taking an average. The XPS spectra was analysed by the CasaXPs software. To determine the films' thicknesses, the AFM technique was used in tapping mode, to measure the height of the step created during fabrication. For both film sets, three different film thicknesses were studied: $<$300 nm, ~450 nm and $>$600 nm.

The morphology of the films was determined using x-ray diffraction (XRD) on a Bruker D2 phaser system. The x-ray generator was at 30 kV and 10 mA. The $2\theta$ range was from 32 to 55° to avoid the silicon peak at 61.7°, with a step size of 0.02° and a scan speed of 0.1 deg $min^{-1}$. The crystallite size was determined using Scherrer equation [41]. Nanoindentation measurements of the FeSiB and FeGaSiB films were carried out using the nanoindentation technique with a Berkovich diamond tip [42, 43]. The load was applied perpendicular to the surface. Arrays of four indents were made at distances 5 μm and 2 μm respectively with a maximum load of 10 mN for 50 cycles, this was repeated at least 14 times per film, with the error bars determined from the standard deviation of the results. The data were analyzed using the Oliver and Pharr method [44, 45], at room temperature.

## 4. Results

The results are presented for the structural and mechanical properties of FeSiB and FeGaSiB films on silicon and glass substrates as a function of thickness.

### 4.1. Structural properties

As the films studied in this work are thicker than previous studies [28, 29], the morphology was determined using XRD. Figure 2 presents the XRD for both film sets (FeSiB and FeGaSiB) for the different film thicknesses. It is observed that all the films had a very broad peak around $2\theta \sim 44°$, which indicated the absence of any periodical atomic arrangement. The FeGaSiB diffused peaks shift to lower angles compared to the FeSiB peaks, which suggests lattice expansion within the FeGaSiB films due to the addition of Ga (table 1). The magnitude of these peaks increased with increasing film thickness. This increase could be due to the formation of nanocrystalline grains within the amorphous matrix in the thicker films. Also as no sharp crystalline peaks were observed, this confirms the amorphous or nanocrystalline nature of all the films studied. Plus the ability to

**Table 1.** Structural properties of the FeSiB and FeGaSiB films determined from the XRD data.

| | 2θ (°) | 2θ peak height | Full width at half max (FWHM) (°) | Crystallite Size (nm) |
|---|---|---|---|---|
| 290 nm FeSiB | 44.5 | 3.85 | 5.51 | 1.6 |
| 425 nm FeSiB | 45 | 5.85 | 5.01 | 1.7 |
| 668 nm FeSiB | 44.4 | 9.07 | 4.97 | 1.7 |
| 283 nm FeGaSiB | 44.3 | 4.73 | 5.41 | 1.6 |
| 450 nm FeGaSiB | 43.9 | 9.79 | 4.81 | 1.8 |
| 640 nm FeGaSiB | 43.8 | 14.79 | 4.56 | 1.9 |

maintain amorphicity at larger thicknesses for these compositions. From the XRD data for each thickness (figure 2), the Scherrer equation [41] was used to determine the average crystallite size within each film, by fitting a Gaussian to the large amorphous peak in Fityk [46]. From table 1, it is observed that the crystallite size for all films was less than 2 nm, hence the films can be taken to have nanocrystallites within an amorphous matrix.

The 2θ peak height can be in part taken as an indicator of the amorphicity of the films, as the lower the height, the more amorphous the film, as there will be fewer nanocrystallites within it. Therefore, as predicted from the enthalpy of mixing, the FeSiB films are more amorphous than the FeGaSiB films, as their comparable peak heights are about ∼60% smaller. This is roughly the same percentage as the difference in the enthalpy of mixing between the two compositions. Further from table 1, the 2θ peak shifts to a lower angle as a function of thickness for the FeGaSiB films. Converting the 2θ into a lattice constant using Bragg's law and assuming a BCC phase, gives values of ∼2.89 Å for 283 nm film, ∼2.91 Å for the 450 nm film and ∼2.92 Å for the 640 nm film, while the FeSiB films have a lattice constant ∼2.88 Å. Thus, the FeGaSiB lattice is expanding as the thickness is increased, which is due to the reduction in inhomogeneous stress within the films [29]. The lattice constants are slightly larger than the crystalline lattice constant of heat-treated BCC FeGaSiB films (∼2.89 Å) [47] and the lattice constant of 800 nm Fe-Ga films (range 2.88 to 2.9 Å) [48], likely to be due to the amorphous morphology and the Ga and B having a positive enthalpy of mixing, so causing an expansion in the lattice. For the FeSiB films, there is no trends within the 2θ peak and hence the lattice constant (all ∼ 2.88 Å), this is likely to be due to the films being more amorphous. This also suggests that the large Ga atoms in the FeGaSiB films plays an important role in the amorphicity and structure of the films. The crystallite size decreases with decreasing thickness for both FeSiB and FeGaSiB. A reduction in entropy with increasing thickness means that the films would be more crystalline with increasing thickness and hence possess a larger crystallite size—this agrees with the experimental results.

### 4.2. Mechanical properties: effect of film thickness

Figure 3 presents the experimental load-displacement curves for the two thickest films and a silicon substrate. The differences between the three curves are due to the differences in the mechanical properties of the three materials. The three curves have different indentation depths (given by the displacement in figure 3), which increase with increasing applied load up to the maximum value ($h_{max}$). For the three materials, the Si substrate had the lowest penetration depth of ∼210 nm, followed by the FeSiB film of ∼300 nm, with the FeGaSiB film having the largest penetration depth of ∼370 nm. Thus, there is a difference between the maximum penetration depths of the FeSiB and FeGaSiB films of ∼70 nm, which is likely to be due to the Ga addition. Adding the Ga within the FeSiB films changes the distribution of the atoms within the film, due to the Ga atoms having a large radius (136 pm) compared to Si (111 pm) and B (87 pm), and Ga having a less negative enthalpy of mixing with the other elements. This leads to a lower amorphicity of the film, which has led to a larger penetration depth.

Figure 4 compares the hardness, $H_r$ and the Young's modulus, $E_s$ of both the FeSiB and FeGaSiB films as a function of displacement for the different thickness films. It is observed that there are three different behaviours observed as a function of thickness. For the thinnest FeSiB (290 nm) film, both the hardness and the Young's modulus decreased with increasing indentation depth up to 100 nm, where the values plateau out to 10 GPa and 155 GPa respectively. This decrease is due to the indentation size effect, hence the hardness and Young's modulus were determined from the displacement depths greater than 120 nm for all the measurements, to avoid this effect. For the 425 nm FeSiB film, and the 283 nm and 450 nm FeGaSiB films, the hardness gradually increased with increasing indentation depth, which was because of the substrate. For both the thickest films (688 nm FeSiB and 640 nm FeGaSiB), after the initial indentation depth, the hardness and the Young's modulus were approximately constant with increasing displacement, meaning the properties were not affected by the substrate or the indentation size. As the substrate seems to affect the thinner films, the mechanical properties of the Si substrate were measured. Table 2 provides an overview of all these measurements. It is observed that the Si substrate has a higher hardness and Young's modulus than all the films studied. Also, the hardness and

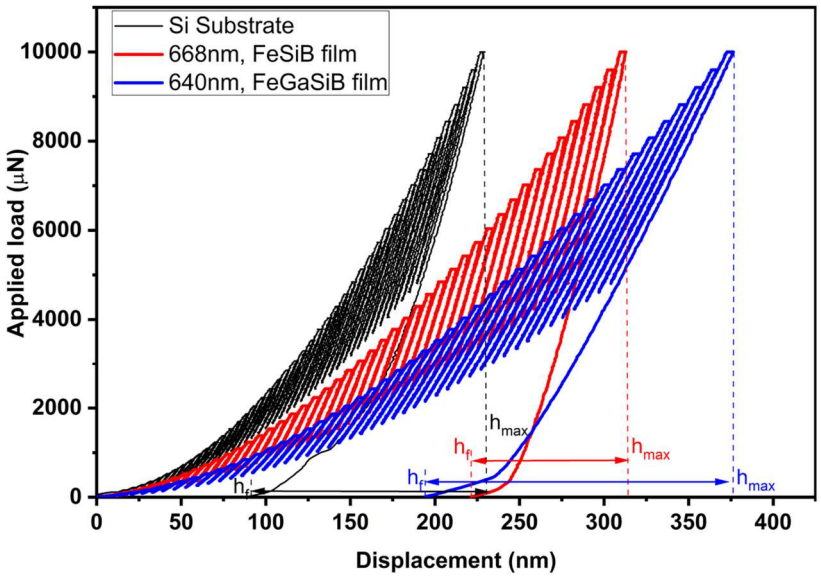


**Figure 3.** Experimental load-displacement curve of partial load function method with 50 cycles as a function of displacement (indentation depth) for the Si substrate, 668 nm FeSiB film and 640 nm FeGaSiB film. The dashed coloured lines and arrows indicate the $h_f$ and $h_{max}$ for the substrate and the films studied.

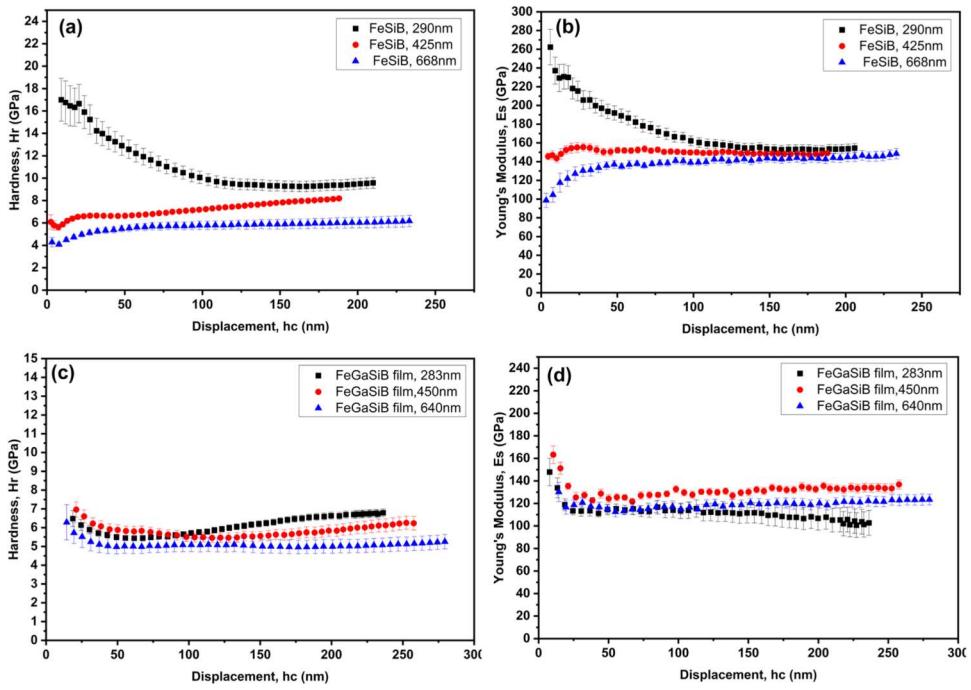


**Figure 4.** Comparison of hardness and Young's modulus of (a) & (b) FeSiB and (c) & (d) FeGaSiB films as a function of thickness and displacement (indentation depth).

Young's modulus decrease as the film thickness increases, confirming that the substrate does affect the mechanical properties of thinner films. The addition of Ga also decreased the hardness and Young's modulus with respect to the FeSiB films, thus reducing the elasticity of the films.

Another parameter obtained from figure 3 is the ratio between the final indentation depth, $h_f$ and the maximum penetration depth at maximum load, $h_{max}$. There is a natural limitation of this ratio between zero and one ($0 \leqslant h_f/h_{max} \leqslant 1$), and it can be used to determine the type of behavior i.e. elastic or plastic. When $h_f/h_{max} = 0$, the deformation is fully elastic and when $h_f/h_{max} = 1$, the deformation is fully plastic. From figure 5, it is observed that as the film thickness increased the ratio of $h_f/h_{max}$ increased. This means that the deformation becomes more plastic as the film thickness increases. Also, the FeGaSiB films had greater plastic deformation

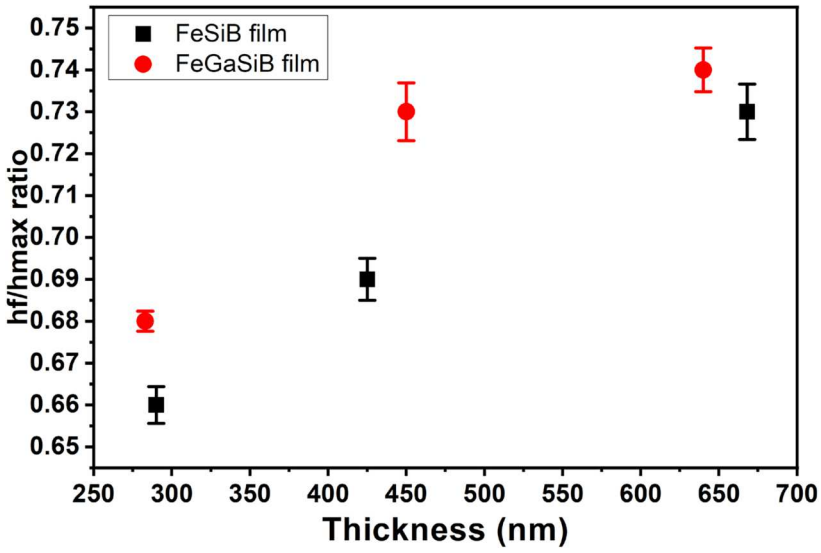


**Figure 5.** The ratio of $h_f/h_{max}$ for the FeSiB and FeGaSiB films grown on silicon as a function of thickness.

**Table 2.** Mechanical properties of different thickness FeSiB and FeGaSiB films, and the silicon substrate.

| | Hardness, $H_r$ (GPa) | Young's Modulus, $E_s$ (GPa) |
|---|---|---|
| Silicon Substrate | 12 | 160 |
| 290 nm FeSiB | 9 | 155 |
| 425 nm FeSiB | 8 | 150 |
| 668 nm FeSiB | 6 | 140 |
| 283 nm FeGaSiB | 7 | 140 |
| 450 nm FeGaSiB | 6 | 130 |
| 640 nm FeGaSiB | 5 | 120 |

compared to the FeSiB films for all thicknesses. The data presented in figure 5 is the average $h_f/h_{max}$ of the 14 nanoindentation measurements made on each film.

### 4.3. Mechanical properties: effect of substrate

Another important factor in thin film growth, is the substrate onto which the film is grown. Previous work has shown that the substrate can affect both the structure and magnetic properties of amorphous films [49], therefore it is important to determine whether the substrate also influences the mechanical properties. To study this, the thickest FeSiB and FeGaSiB films were grown on silicon (a harder substrate) and glass (a softer substrate), and the mechanical properties were determined.

Figure 6 shows how the hardness and Young's modulus change as a function of displacement for the thicker FeSiB and FeGaSiB films grown on silicon and glass substrates. For the hardness (figure 6(a)), the 668 nm FeSiB films on silicon and glass had the same hardness of 6 GPa within error, for indentation depths greater than 50 nm. Similarly for the 640 nm FeGaSiB films the hardness was ~5 GPa for both films, within the error of the measurement. From [50], the hardness of glass is 6.8 GPa, so slightly higher than both the amorphous films. Thus the hardness of both FeSiB and FeGaSiB films were independent of the substrate they were grown on, due to the thickness of the films being larger than the indentation penetration depth.

While for the Young's modulus of the films, there is a strong dependence on the substrate (figure 6(b)), with the values diverging from each other with increasing indentation depth and applied load. For both films grown on silicon, the Young's modulus was approximately constant for indentation depths greater than 100 nm, with the FeSiB/Si film Young's modulus ~140 GPa and the FeGaSiB/Si film Young's modulus ~120 GPa. However, for both films grown on glass, the Young's Modulus decreased with increasing indentation depth. For the FeSiB/glass film the Young's modulus decreased from 130 GPa to 80 GPa, and for the FeGaSiB/glass film, the decrease was from 100 GPa to 70 GPa, then it was approximately constant for indentation depths greater than 200 nm. From [49], the Young's modulus of glass is 73 GPa, thus the Young's modulus of the FeSiB and

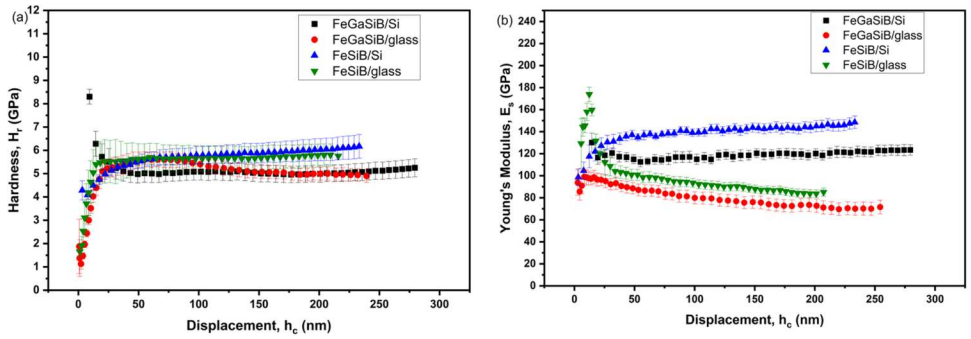


**Figure 6.** Comparison of (a) hardness and (b) Young's Modulus of 668 nm FeSiB and 640 nm FeGaSiB films deposited on Si and glass substrates as a function of displacement.

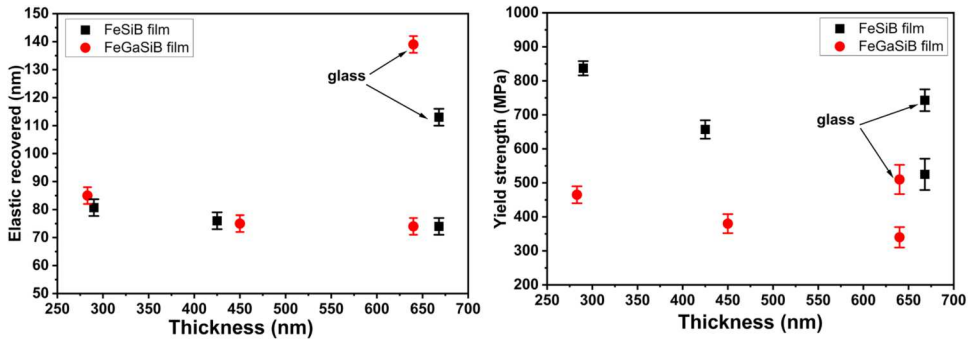


**Figure 7.** (a) Elastic recovery and (b) yield strength of FeSiB and FeGaSiB films deposited on Si and glass substrates as a function of film thickness.

FeGaSiB films grown on glass reduce towards the glass value. Hence the films were strongly affected by the elastic properties of the glass substrate. This means that the amorphous films showed different elastic behaviour depending on whether they were grown on an amorphous substrate (glass) or a crystalline substrate (Si).

Another parameter that can be determined from figure 3, is the elastic recovered part of the material. This is due to part of the film moving back into position once the indentation tip has been removed from the film. It is defined as the difference between the maximum indentation depth, $h_{max}$ and the final indentation depth, $h_f$. From figure 7(a), it is observed that for both films the elastic recovered part decreased with increasing film thickness but was independent of film composition. For the thicker films grown on glass, the elastic recovery is higher than those grown on silicon, again demonstrating that the elastic behaviour of amorphous films strongly depends on the substrate.

The yield strength [51] (figure 7(b)) was also determined for both film sets as a function of thickness and substrate. From figure 7(b), it is observed that the yield strength decreases as the film thickness increases for both film sets. Also, all the FeGaSiB films had a lower yield strength than the FeSiB films, meaning that adding Ga to the films reduced the elasticity within the films. This is because the yield strength is the point, which separates the elastic and plastic behaviour of the film. Again, the yield strength of both the FeSiB and FeGaSiB films were strongly affected by the substrate, with the FeSiB and FeGaSiB films grown on glass having a yield strength ~1.5 times larger than those grown on silicon. Thus the softer glass substrate increases the elasticity within the amorphous films compared with the hard silicon substrate.

The hardness and elastic modulus can also be affected by the materials itself: either a pile-up or a sink-in or both, which occurs on the sides of the indented edges. To study this, AFM images and cross-sectional lines were taken (figure 8). For both the FeSiB films on silicon and glass, a small pile-up of material on three sides is observed (shown by the arrows on figures 8(b) and (d)). The pile-up height of FeSiB/Si was in the range 12–19 nm and for FeSiB/glass was in the range 13–16 nm. Thus as they have similar pile-up heights, the substrate has not influenced the measurement. Hence the pile-up is purely the behaviour of the FeSiB film, and due to the lack of compressibility of the plastic deformation [20]. For the FeGaSiB film on silicon, the pile-up material height on one side of the indent profile (black arrows in figure 8(f)) is 26 nm, which is double that of the FeSiB film on silicon. While the FeGaSiB film on glass does not show a pile-up effect at all, as all the heights are level (figure 8(h)) and parallel to the original surface. This means the substrate plays a role in the compressive stress within the FeGaSiB films.

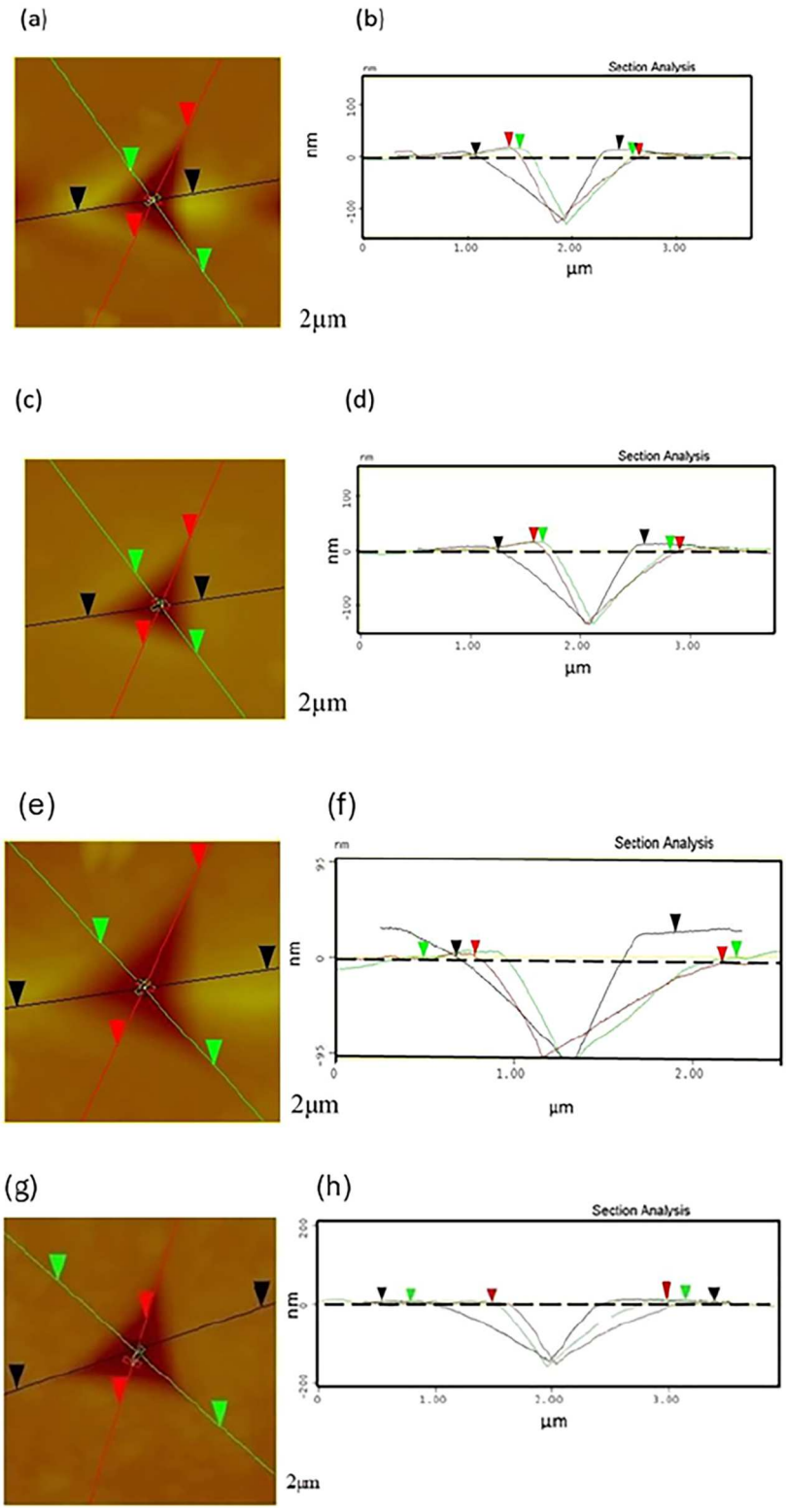


**Figure 8.** Indent surface features and section analysis, AFM image (2 × 2 µm) and section analysis of 640 nm FeSiB film on a Si substrate (a) and (b) and a glass substrate (c) and (d) and 640 nm FeGaSiB film on a Si substrate (e) and (f) and a glass substrate (g) and (h).

## 5. Discussion

### 5.1. Hardness of the films

From table 2, it is observed that the hardness and Young's Modulus decreased with increasing thickness for both film sets, with the thinnest film values being closer to those of the silicon substrate. For the films with thicknesses greater than 600 nm, the substrate did not influence the properties, while as the thickness got thinner, the substrate effect got larger. Comparing the hardness with those measured for FeSiB ribbons [20], it

is observed that the ribbons hardness was double (10 GPa) compared to the films (6 GPa). The reduced modulus of FeSiB ribbons is given as ~160 GPa. The reduced modulus is measured in the nanoindentation measurement, before being converted into the Young's modulus. Thus the reduced modulus of the >600 nm films on silicon were ~135 GPa (FeSiB) and ~115 GPa (FeGaSiB) [52], which again are lower than the ribbons. The main reason why thin films mechanical properties are different to ribbons is due to the different in manufacturing method. For thin films, sputtering can induce strain into the films, which influences the properties, while ribbons are produced using rapid melt spinning. This means that it cannot be assumed that thin films of materials will have the same properties as the bulk or ribbon samples.

For comparison with other magnetostrictive thin films, Nicolenco *et al* [23] investigated electrodeposited Fe-Ga films (thickness >600 nm), as a function of Ga concentration. The hardness ranged from 5 GPa (2% Ga) to 2.93 GPa (35% Ga), while the reduced modulus ranged from 134 GPa (2% Ga) to 115 GPa (35% Ga). Comparing to the amorphous FeGaSiB films, where the Ga content is 7%, the hardness for thinner films is higher than the polycrystalline Fe-Ga films, while the 640 nm FeGaSiB film hardness is in good agreement with the 2% Ga film. While the reduced modulus for the 640 nm FeGaSiB film is closer to the higher content Ga films, with the 668 nm FeSiB film having a reduce modulus the same as the 2% Ga film. Therefore, both amorphous FeSiB and FeGaSiB films have comparable mechanical properties with polycrystalline Fe-Ga films. Further it suggests that amorphous magnetostrictive films have higher hardness compared to polycrystalline magnetostrictive films, which is the same behaviour as observed between bulk amorphous glasses and polycrystalline alloys [38]. While the reduced modulus and hence the Young's modulus is reduced for amorphous magnetostrictive films, compared to polycrystalline films.

### 5.2. Effect of Ga addition

The addition of Ga to the FeSiB films, also changed the mechanical properties of the amorphous films. Previous work on non-magnetic films, found that increasing the internal tensile stress leads to a decrease in both the hardness and elastic modulus [40]. For example, increasing the internal stress by 1 GPa leads to a decrease in the elastic modulus of about 13% [53]. While work by Qunito *et al* [54] and Mani *et al* [55] found that increasing the compressive stress within the film increased the hardness. As the deposition of the FeSiB and FeGaSiB films were carried out using the same growth conditions, any changes in the internal stress within the films, will be due to the addition of the Ga, rather than the growth parameters (i.e. sputter power and pressure). From the XRD data (table 1), it is observed that the estimated lattice constants increased with FeGaSiB film thickness, which can be linked to an increase in tensile stress, which would then explain the decrease in the hardness and elastic modulus measured.

Previous work on FeGaSiB films [29] determined that the addition of Ga to FeSiB films, decreased the inhomogeneous stress within the films, due to the larger Ga atom increasing the spacing between the other atoms within the film. This is also observed in these films (table 1). This reduction in stress within the FeGaSiB films, is therefore likely to be the reason for the decrease in the hardness and Young's modulus observed. The addition of Ga to FeSiB reduced the elasticity of the films, as observed in figures 5 and 7(b). The reduction in yield strength (figure 7(b)) and increase in plasticity (figure 5), is likely to be due to the Ga changing the short range atomic spacing within the amorphous films.

### 5.3. Effect of substrate

From figures 6(b)–8, the effect of the substrate on the mechanical properties of the amorphous FeSiB and FeGaSiB films is observed. It is important to understand the role the substrate plays in the overall properties of the films if they are going to be used in MEMS applications. The thickest films were studied on the different substrates, as the hardness and Young's modulus were not affected by the silicon in the previous measurement. The hardness (figure 6(a)) was also not affected by the substrate, as the values were the same for both substrates, but the substrate the amorphous films were grown on did strongly influence the measured Young's modulus (figure 6(b)). Although it had been determined that the 600 nm films were not affected by the silicon substrate, the growth on the glass substrate had a strong effect on the measured Young's modulus. This means that the mechanical behaviour of the amorphous films depends on whether the Young's modulus of the substrate is higher or lower than the film.

Previous modelling, [56] demonstrated that the mechanical properties of the substrates can influence the films properties over different depth ranges. This is due to the substrate starting to elastically deform at smaller penetration depths than expected. The larger the difference between the Young's modulus of the film ($E_f$) and the substrate ($E_s$), given by $E_f/E_s$, the greater the effect. If $E_f/E_s = 1$, then no effect of the substrate is observed, while for harder substrates (i.e. $E_f/E_s < 1$), the Young's modulus tends towards the substrate value but does not reach it. For $E_f/E_s > 2$, i.e. softer substrates, the Young's modulus tends towards the substrate value and is a stronger effect. This is observed in our films, where the >600 nm films on silicon showed no effect of the silicon properties, with $E_f/E_s = 0.875$ (FeSiB) and

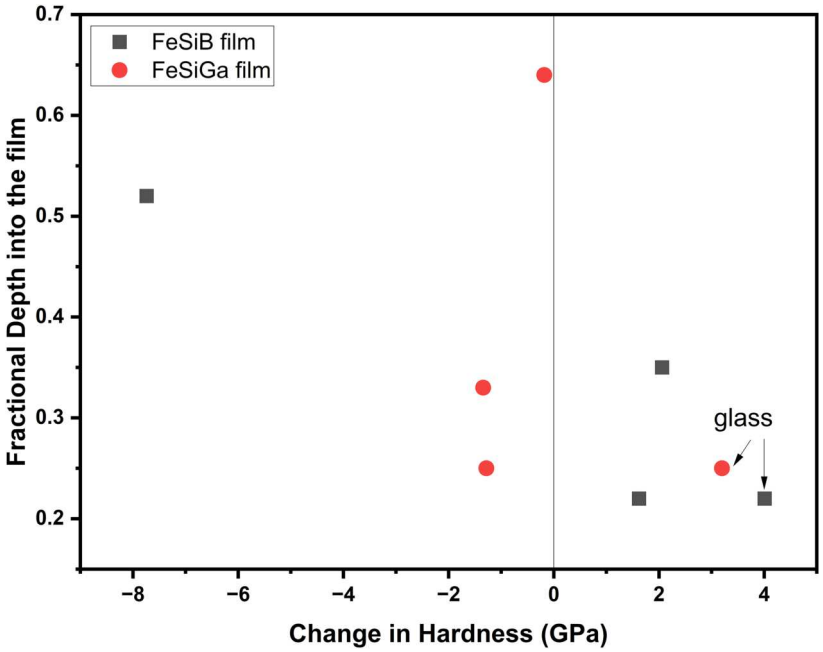


**Figure 9.** Fractional depth ratio as a function of the change in hardness within the FeSiB and FeGaSiB films.

0.75 (FeGaSiB), so both being close to one. While for the same thickness films on glass, there was a stronger dependence on the glass substrate, with $E_f/E_s$ of 1.92 (FeSiB) and 1.64 (FeGaSiB). Thus this larger ratio and the glass having softer properties, caused a greater effect in the Young's modulus measurement.

### 5.4. Effect of film thickness

The substrate and film thickness also affected the elasticity and yield strength of the films (figure 7). Previous work on the yield strength ($\sigma_y$) found that for Cu films grown on kapton substrate, the yield strength decreased with film thickness, according to the relation [57]:

$$\sigma_y = \sigma_o + kd^{-n} + k't^{-m} \tag{1}$$

Where $\sigma_o$ is the bulk yield strength, $k$ and $k$' are gradients, $d$ is the grain size, $t$ is the film thickness and $n$ and $m$ are exponents. As the FeSiB and FeGaSiB films are amorphous, they contain no grains, thus $d = 0$. This means that the yield strength depends only on the film thickness. This is due to the dislocations in the film being blocked either at the interface between the film and the substrate or at the film surface. Equation (1) was fitted to the data in figure 7(b), and the bulk yield strength and exponent determined for the fitting, which gave the coefficient of determination, $R^2$ closes to 1, due to there being only 3 data points. For the FeSiB films, the bulk yield strength was 278 MPa and the exponent $m = 1$. While for the FeGaSiB films, the bulk yield strength was 242 MPa and the exponent $m = 1$. From previous analysis [58], and plasticity theory [59] it is expected that $m = 1$ for thin films, with any variation due to a heavily stressed layer at the interface. The best fit for both films were $m = 1$, meaning that both films are behaving according to the plasticity theory [59], where the interface between the film and the substrate blocks the dislocations within the film, which produces an inhomogeneous strain distribution at the interface. While the films on the glass substrate had a higher yield strength to those on the silicon, this means that the glass was more of a barrier to the dislocations within the film, than the silicon was, thus increasing the inhomogeneous strain distribution and therefore the yield strength.

### 5.5. Amorphicity and thickness variations

Since metallic glasses have a higher yield strength and hardness than their crystalline counterparts [38], hardness at different depths can be taken to be representative of the crystallinity of the structure. To quantify this difference and for adequate comparison between compositions, the change in hardness was computed for both compositions at the film surface (displacement $<10$ nm) and a depth of 160 nm. Negative values show that the material becomes softer the deeper it goes, i.e. more crystalline within the film, while positive values show that the material becomes harder the deeper it goes, i.e. more crystalline at the surface. This naïve analysis gives an indication if for a particular thickness, the surface is more amorphous (or more crystalline) than at 160 nm into the film. The fractional depth of the thin film can be represented as the ratio of the depth to the film thickness. A biplot of the fractional depth against change in hardness is shown in figure 9, where the different

behaviours between the FeSiB and FeGaSiB films is observed. For the FeGaSiB films, there is a small negative change in hardness between the surface and the inside of the films, meaning the inside of the films has a slightly lower hardness, but there is no real change in morphology from the surface into the film. For the FeSiB films, the thinnest film has a large negative change from the surface compared to inside the film, suggesting that the morphology is different between the two and the interface between the Si substrate and the film is still influencing the growth. While the thicker two FeSiB films have a positive change, suggesting that the inside of the films was more amorphous than the surface. For both the FeSiB and FeGaSiB films, the change in hardness for the two thicker films is similar, which suggests that the interface has stopped influencing the film's morphology at thicknesses greater than 300 nm. For the thickest films grown on glass, both the FeSiB and FeGaSi films had a larger positive change compared to the films grown on silicon, this suggests that both films were more amorphous within the film than at the surface, and that the entropy associated with the glass-film interface is still strongly influencing the film growth, especially for the FeGaSiB film.

## 6. Conclusions

The mechanical properties (hardness, Young's modulus and yield strength) have been investigated for amorphous FeSiB and FeGaSiB films, to determine how the film thickness, composition and substrate affect these properties. The addition of Ga into the films changed the mechanical properties, with the films becoming less elastic, this is likely to be due to the Ga changing the internal stress within the films, which is observed by the change in the amorphous peak position in the XRD data. While the harder silicon substrate did not affect the measurements of the thickest films, the softer glass substrates had a large influence over the measured values. The FeSiB film hardness and Young's modulus also differed from those of ribbons, meaning that the mechanical properties of thin films used in MEMS applications must be fully characterised, rather than assume that they are the same as the bulk/ribbon values.

Additionally, the amorphicity of the films was approximated using Scherrer crystallite size analysis, i.e. nanocrystallites formed within an amorphous matrix. By comparing this to the hardness data obtained (as a function of thickness) it was inferred that the FeGaSiB films were slightly more amorphous at the surface, while the thicker FeSiB films were more amorphous within the film. Taken in combination, the data shows that (a) film growing parameters can contribute to a staggered distribution of particle sizes that can affect thin film physical properties, and (b) this characteristic can be used as an additional lever into the design and customisation of functional magnetic thin films.

## Acknowledgments

The authors would like to acknowledge the Iraqi Ministry of Higher Education & Scientific research for the financial support on this project. Also, the authors would like to acknowledge Dr David Morgan, for the XPS data collection, which was performed at the EPSRC National Facilities for XPS ('HarwellXPS'), operated by Cardiff University and UCL, under contract No. PR16195.

## Conflicts of interest

The authors declare no conflict of interest.

## Data availability statement

All data that support the findings of this study are included within the article (and any supplementary files).

## Funding

This research was funded by the Iraqi Ministry of Higher Education & Scientific research.

## Author contributions

Zhaoyuan Leong
Formal analysis (supporting), Writing – review & editing (equal)

Saturi Baco
Writing – original draft (supporting)

Nicola A Morley 0000-0002-7284-7978
Conceptualization (equal), Funding acquisition (lead), Project administration (lead), Supervision (lead), Validation (supporting), Writing – original draft (supporting), Writing – review & editing (equal)

## References

[1] Liang X, Dong C, Chen H, Wang J, Wei Y, Zaeimbashi M, He Y, Matyushov A, Sun C and Sun N 2020 A review of thin-film magnetoelastic materials for magnetoelectric applications *Sensors* **20** 1532
[2] Herrera-May A L, Soler-Balcazar J C, Vazquez-Leal H, Martinez-Castillo J, Vigueras-Zuniga M O and Aguilera-Cortes L A 2016 Recent advances of MEMS resonators for lorentz force based magnetic field sensors: design, applications and challenges *Sensors* **16** 1359
[3] Endo Y, Sakai T, Miyazaki T and Shimada Y 2017 Effect of film thickness on the high frequency magnetic properties of polycrystalline Fe-Ga films *IEEE Trans. Mag.* **53** 1–5
[4] Jen S U, Tsai T L, Li M S, Kuo P C and Lin M Y 2011 Magnetic properties of Fe62Co19Ga19 films deposited on Si(100) substrates *J. Appl. Phys.* **109** 07A920
[5] Morley N A, Rigby S and Gibbs M R J 2009 Anisotropy and magnetostriction constants of nanostructured Fe50Co50 films *J. Optoelectron. Adv. Mater. Symp* **1** 109–13
[6] Khan M M, Nemati A, Rahman Z U, Shah U H, Asgar H and Haider W 2017 Recent advancements in bulk metallic glasses and their applications: a review *Crit. Rev. Solid State Mater. Sci.* **43** 233–68
[7] Hashimoto Y, Yamamoto N, Kato T, Oshima D and Iwata S 2017 Spin-valve giant magneto-resistance film with magnetostrictive FeSiB amorphous layer and its application to strain sensors *J. Appl. Phys.* **123** 113903
[8] Sun Z G, Kuramochi H, Mizuguchi M, Takano F, Semba Y and Akinaga H 2004 Magnetic properties and domain structures of FeSiB thin films *Surf. Sci.* **556** 33–338
[9] Diguet G, Makabe K, Froemel K, Kurita H, Narita F and Muroyama M 2022 Magnetic properties of Fe-Si-B thin films and their application as stress sensors *Thin Sold Films* **758** 139428
[10] Kurita H, Diguet G, Froemal J and Narita F 2023 Stress sensor performance of sputtered Fe-Si-B alloy thin coating under tensile and bending loads *Sensors Actuators* A **343** 113652
[11] Liu Y, Sang S, Zhao D, Ge Y, Xue J, Duan Q and Guo X 2024 Novel flexible magnetoeleastic biosensor based on PDMS/FeSiB/QD composite film for the detection of African swine fever virus P72 protein *Anal. Methods* **16** 5441–9
[12] Turutin A V *et al* 2023 Magnetoelastic MEMS magnetic field sensor based on laminated heterostructure of bidomain lithium niobate and metglas *Materials* **16** 484
[13] Patil D R, Kumar A and Ryu J 2021 Recent progress in devices based on magnetoelectric composite thin films *Sensors* **21** 8013
[14] Röbisch V, Salzer S, Urs N O, Reermann J, Yarar E, Piorra A, Kirchhof C, Lage E, Höft M and Schmidt G U 2017 Pushing the detection limit of thin film magnetoelectric heterostructures *J. Mater. Res.* **32** 1009–19
[15] Karampuri Y, Wang Y and Wu T 2022 Ferromagnetic resonance and spin-wave exchange stiffness of FeGaB/$Al_2O_3$ multilayer thin film stack for microwave applications *Mater. Chem. Phys.* **279** 125776
[16] Zaeimbashi M *et al* 2021 Ultra-compact dual-band smart NEMS magnetoelectric antennas for simultaneous wireless energy harvesting and magnetic field sensing *Nat. Commun.* **12** 3141
[17] Zhang Q and Zhu Z 2022 A flexible force-sensitive film with ultra-high sensitivity and wide linear range and its sensor *J. Alloys Compd.* **895** 162026
[18] Garcia M A, Elabaile L, Torres Y, Crespo R D, Carrizo J and Garcia J A 2018 Microstructure and room temperature mechanical properties of crystalline and amorphous FeAl based melt spun ribbons *J. Non-Cryst. Sol.* **497** 1–6
[19] Lashgari H R, Cadogan J M, Chu D and Li S 2016 The effect of heat treatment and cyclic loading on nanoindentation behaviour of FeSiB amorphous alloy *Mater. Design* **92** 919–31
[20] Lashgari H R, Chen Z, Liao X Z, Chu D, Ferry M and Li S 2015 Thermal stability, dynamic mechanical analysis and nanoindentation behaviour of FeSiB(Cu) amorphous alloys *Mater. Sci. Eng.* A **626** 480–99
[21] Jen S U, Tsai T L, Kuo P C, Chi W L and Cheng W C 2010 Magnetostrictive and structure properties of FeCoGa films *J. Appl. Phys.* **107** 013914
[22] Baco S, Abbas Q A, Hayward T J and Morley N A 2021 An Investigation on the mechanical properties of soft magnetostrictive FeCoCr films by nanoindentation *J. Alloys. Comp.* **881** 160549
[23] Nicolenco A, Chen Y, Tsyntsaru N, Cesiulis H, Pellicer E and Short J 2021 Mechanical, magnetic and magnetostrictive properties of porous Fe-Ga films prepared by electrodeposition *Mater. Des.* **208** 109915
[24] Roas S, Sirena M, Domenichini P and Abarzua G 2025 AFM nanoindentation-based study of thickness effects on the pseudoelastic behaviour of Ni-Mn-Ga thin films *Chem. Phys. Lett.* **874-875** 142171
[25] Takhsha Ghahfarokhi M, Casoli F, Minnert C, Bruns S, Bruder E, Cabassi R, Durst K, Gutfleisch O and Albertini F 2023 Effects of nanoindents on the martensitic transformation of Ni-Mn-Ga shape-memory Heusler films: a study by high-resolution imaging as a function of temperature *Acta Mater.* **245** 118603
[26] Liu W-J, Chang Y-H, Hsu S-T, Fern C-L, Chen Y-T, Tsao S-Y and Lin S-H 2024 Exploring the correlation between surface roughness, surface energy, nano-indentation, electrical properties, and magnetic characteristics of annealed $Co_{40}Fe_{40}Dy_{20}$ thin films deposited on Si(100) substrates *J. Electron. Mater.* **53** 4498–511
[27] Fern C-L, Liu W-J, Chang Y-H, Chiang C-C, Chen Y-T, Lu P-X, Su X-M, Lin S-H and Lin K-W 2023 Surface roughness-induced changes in important physical features of CoFeSm thin films on glass substrates during annealing *Materials* **16** 6989
[28] Abbas Q A and Morley N A 2017 Fabrication and characterisation of magnetostrictive amorphous FeGaSiB thin films *J. Magn. Magn. Mater.* **439** 353–7
[29] Abbas Q A, Thomson T, Hayward T J and Morley N A 2020 Influence of Ga evaporation rate on the magnetic properties of Amorphous FeGaSiB thin films *J. Magn. Magn. Mater.* **498** 166160
[30] Hattrick-Simpers J R *et al* 2008 Combinatorial investigation of magnetostriction in Fe–Ga and Fe–Ga–Al *Appl. Phys. Lett.* **93** 102507

[31] Takeuchi A and Inoue A 2010 Mixing enthalpy of liquid phase calculated by Miedema's scheme and approximated with sub-regular solution model for assessing forming ability of amorphous and glassy alloys *Intermetallics* **18** 1779–89
[32] Leong Z, Huang Y, Goodall R and Todd I 2018 Electronegativity and enthalpy of mixing biplots for high entropy alloy solid solution prediction *Mater. Chem. Phys.* **210** 259–68
[33] He Q and Tang Y 2018 On lattice distortion in high entropy alloys *Frontiers In Materials* **5** 42
[34] Takeuchi A and Inoue A 2005 Classification of bulk metallic glasses by atomic size difference, heat of mixing and period of constituent elements and its application to characterisation of the main alloying element *Mater. Trans.* **46** 2817–29
[35] Jones A O F, Chattopadhyay B, Geerts Y H and Resel R 2016 Substrate-induced and thin film phases: polymorphism of organic materials on surfaces *Adv. Funct. Mater.* **26** 2233–55
[36] Thompson G B 2003 Predicting polymorphic phase stability in multilayer thin films *PhD Thesis* The Ohio State University
[37] Kashchiev D 2000 *Nucleation: basic theory with applications* 1 1st edn (Butterworth Heinemann)
[38] Greer A L 2009 Metallic glasses … on the threshold *Mater. Today* **12** 14–22
[39] Haneczok G, Madej L, Chrobak A, Kwapulinski P, Stoklosa Z and Rasek J 2010 Influence of free volume on magnetoelastic coupling in iron-based amorphous materials *Phys. Scr.* **81** 025702
[40] Morley N A, Yeh S-L, Rigby S, Javed A and Gibbs M R J 2008 Development of a cosputter-evaporation chamber for Fe-Ga films *J. Vac. Sci. Technol.* **26** 581
[41] Hammond C 2009 *The Basics of Crystallography and Diffraction* 3rd edn (Oxford University Press)
[42] Sasaki Y, Ciappa M, Masunaga T and Fichtner W 2010 Accurate extraction of the mechanical properties of thin films by nanoindentation for the design of reliable MEMS *Microelectron. Reliab.* **50** 1621–5
[43] Pharr G M and Oliver W C 1992 Measurement of Thin film mechanical properties using nanoindentation *MRS Bull.* **17** 28–33
[44] Oliver W C and Pharr G M 2004 Measurement of hardness and elastic modulus by instrumented indentation: Advances in understanding and refinements to methodology *J. Mater. Res.* **19**
[45] Oliver W C and Pharr G M 1992 An improved technique for determining hardness and elastic modulus using load and displacement sensing indentation experiments *J. Mater. Res.* **7** 1564–83
[46] Wojdyr M 2010 Fityk: a general purpose peak fitting program *J. Appl. Cryst.* **43** 1126–8
[47] Abbas Q A, Rodrigues M, Baco S, Guan S and Morley N A 2020 Influence of annealing temperature on the structural and magnetic properties of FeGaSiB thin films *Thin Solid Films* **701** 137955
[48] Dunlap R A, Deschamps N C, Mar R E and Farrell S P 2006 Mossbauer effect studies of $Fe_{100-x}Ga_x$ films prepared by combinatorial methods *J. Phys. Condens. Matter* **18** 4907
[49] Carabias I, Martinez A, Garcia M A, Pina E, Gonzalez J M, Hernando A and Crespo P 2005 Magnetostrictive thin films prepared by RF sputtering *J. Magn. Magn. Mats* **290-291** 823–5
[50] Saha R and Nix W D 2002 Effects of the substrate on the determination of thin film mechanical properties by nanoindentation *Acta Mater.* **50** 23–38
[51] Giannakopoulos A E and Suresh S 1999 Determination of elastoplastic properties by instrumented sharp indentation *Scr. Mater.* **40** 1191–8
[52] Abbas Q A 2019 Magnetic and mechanical properties of magnetostrictive FeGaSiB Films *PhD Thesis* University of Sheffield
[53] Chuang C T, Chao C K, Chang R C and Chu K Y 2008 Effect of internal stresses on the mechanical properties of deposition thin films *J. Mater. Proce. Technol.* **201** 770–4
[54] Quinto D T, Santhanam A T and Jindal P C 1988 Mechanical properties, structure and performance of chemically vapor-deposited and physical vapor-deposited coated carbide tools *Mater. Sci. Eng. A* **105–106** 443–52
[55] Mani A, Aubert P, Mercier F, Khodja H, Berthier C and Houdy P 2005 Effects of residual stress on the mechanical and structural properties of TiC thin films grown by RF sputtering *Surf. Coat. Technol.* **194** 190–5
[56] Antunes J M, Fernandes J V, Sakharova N A, Oliveira M C and Menezes L F 2007 On the determination of the Young's modulus of thin films using indentation tests *International J. Solid. Struct.* **44** 8313–34
[57] Yu Denis Y W and Spaepen F 2004 The yield strength of thin copper films on Kapton *J. Appl. Phys.* **95** 2991
[58] Nix W D 1989 Mechanical properties of thin films *Metall. Trans. A* **20** 2216
[59] Fleck N A and Hutchinson J W 1997 Strain gradient plasticity *Advanced Applied Mechanics* **33** 295–361 Academic Press